

S-nitrosylation influences the structure and DNA binding activity of AtMYB30 transcription factor from *Arabidopsis thaliana*

Carolina Pereira Tavares^a, Javier Vernal^a, Ricardo Alexandre Delena^a, Lorenzo Lamattina^b, Raul Cassia^b, Hernán Terenzi^{a,*}

^a Centro de Biología Molecular Estructural-INBEB, Departamento de Bioquímica, CCB, Universidade Federal de Santa Catarina, Florianópolis, Brazil

^b Instituto de Investigaciones Biológicas, Facultad de Ciencias Exactas y Naturales, Universidad Nacional de Mar del Plata, CC1245 (7600) Mar del Plata, Argentina

ARTICLE INFO

Article history:

Received 28 September 2013

Received in revised form 14 February 2014

Accepted 19 February 2014

Available online 26 February 2014

Keywords:

MYB transcription factors

Nitric oxide

Nitrosylation

AtMYB30 DBD

Arabidopsis

Biotin switch assay

ABSTRACT

MYB proteins are a family of transcription factors that play an important role in plant development and regulatory defense processes. *Arabidopsis thaliana* MYB30 (AtMYB30), a member of this protein family, is involved in cell death processes during the hypersensitive response (HR) of plants. HR is characterized by a vast production of reactive oxygen species (ROS) and nitric oxide (NO). NO may thus influence the binding of AtMYB30 to DNA. In this work we evaluated the effect of NO on AtMYB30 DNA binding activity, and also in the protein structural properties. A fully active minimal DNA-binding domain (DBD) of AtMYB30 (residues 11–116) containing two cysteine residues (C49 and C53) was overexpressed and purified. Site-directed mutagenesis was used to obtain AtMYB30 DBD mutants C49A and C53A. The DNA binding activity of AtMYB30 DBD, and Cys single mutants is clearly inhibited upon incubation with a NO donor, and S-nitrosylation was confirmed by the biotin switch assay. Finally, in order to understand the mechanism of NO effect on AtMYB30 DNA binding activity we performed circular dichroism analysis, to correlate the observed protein function inhibition and a potential structural impairment on AtMYB30 DBD. Indeed, NO modification of C49 and C53 residues promotes a subtle modification on the secondary structure of this transcription factor. We thus demonstrated, using various techniques, the *in vitro* effect of NO on AtMYB30 DBD, and thus the potential consequences of NO activity on plant metabolism influenced by this transcription factor.

© 2014 Elsevier B.V. All rights reserved.

1. Introduction

MYB transcription factors play a wide variety of physiological functions in the regulation of gene expression in higher plants including the regulation of primary and secondary metabolism, the control of cell development and the cell cycle, the participation in defense and response to various biotic and abiotic stresses, and hormone synthesis and signal transduction [1–4]. MYB superfamily members are characterized by a highly conserved DNA-binding domain – the MYB domain – which generally comprises up to three imperfect repeats (R1, R2 and R3), each forming a helix–turn–helix structure of about 50–53 amino acids that intercalates into the major groove of DNA [1,5]. MYB proteins can be classified in three subfamilies, according to the number of repetitions in the adjacent region of MYB domain. R2R3-MYBs (with two repetitions) constitute the largest MYB subfamily present exclusively in plants, with 126 members in the model plant *Arabidopsis* [1,6].

Nitric oxide (NO) is an endogenous signal molecule in plants that mediates responses to several stimuli through the post-translational (S-nitrosylation) modification of thiol residues in proteins [7].

Regarding transcription factors (TF), Brendeford and coworkers (1998) reported that NO donors like sodium nitroprusside (SNP) and S-nitrosoglutathione (GSNO) severely reduced the DNA-binding activity of c-Myb, a TF found in vertebrates and identified as the cellular homologue of v-Myb, an oncogene found in two avian retroviruses that induce leukemia [8]. A few years ago our group observed a relationship between the redox state of the R2R3-MYB from *Arabidopsis thaliana* AtMYB2 – influenced by NO donors – and its DNA-binding properties [9]. Furthermore, S-nitrosylation is gaining increasing importance as a key regulatory mechanism during plant stress responses, as well as during changes in the redox potential of the cell [10–12]. The identification of the proteome that can be modulated by S-nitrosylation in plants will certainly contribute to understand the regulation mechanisms and the functional relevance of this process.

The presence of a conserved cysteine residue in the DNA-recognition helix R2, is a typical characteristic of R2R3-MYB DNA binding domains in plants. It was demonstrated that NO donors severely inhibited the DNA-binding activity of c-Myb, and that Cys130 (equivalent to the Cys53 in R2R3 AtMYB) was responsible for this sensitivity to NO [8]. The reduced state of Cys130 is essential for c-Myb DNA-binding [13]. AtMYB30 is a R2R3-MYB TF which acts as a positive regulator of the HR, a form of programmed cell death associated with resistance in

* Corresponding author.

E-mail addresses: hterenzi@ccb.ufsc.br, hterenzi@me.com (H. Terenzi).

adult *Arabidopsis* plants during pathogen attacks [14–18]. AtMYB30 may be regulated by several posttranslational modifications, which activates or repress its transcriptional activity. An interesting and very recent example of positive interaction is that promoted by BES1, a component of the brassinosteroid (BR) signaling pathway. It was reported that AtMYB30 interacts with BES1 both *in vitro* and *in vivo*, inducing BR downstream target genes [15]. Likewise, sumoylation is critical for AtMYB30 function during ABA signaling. The SUMO E3 ligase SIZ1 is required for the sumoylation of AtMYB30 at lysine residue 283, which is critical for AtMYB30 transcriptional activity in response to abscisic acid [19].

On the other hand, some AtMYB30 negative regulators were reported. AtMYB30 and the secreted phospholipase AtsPLA2- α physically interact *in vivo*, as a consequence, AtMYB30 transcriptional activity is repressed, causing down regulation of plant HR [20]. It was also reported that the helix-loop-helix domain of the *Xanthomonas* type III effector xopD interacts with AtMYB30, inhibiting the transcription of MYB30 defense-related target genes, suppressing the *Arabidopsis* defense [21]. Besides, the *Arabidopsis* MIEL1 (MYB30-Interacting E3 Ligase1), ubiquitinates AtMYB30, leading to MYB30 proteasomal degradation and down regulation of its transcriptional activity [16].

In this work, we demonstrate that S-nitrosylation is a negative regulator of AtMYB30 DNA binding activity *in vitro*, and that this posttranslational modification is able to modify the secondary structure, and the thermal stability of the protein. This posttranslational modification is coincident with our report about AtMYB2 inhibition by nitrosylation [9]. Accordingly, a wide array of proteins involved in all major cellular activities were demonstrated to be negatively regulated by S-nitrosylation as GAPDH, NADPH oxidase, NPR1, catalase, metacaspase 9, ascorbate peroxidase, rubisco in *A. thaliana* [22,23].

Thus, the NO-dependent AtMYB30 nitrosylation may provide a mechanism responsible for the turnoff of the biological activity of this regulatory protein after the initial response of plants to stress.

2. Material and methods

2.1. AtMYB30 DBD expression and purification

The cDNA coding for AtMYB30 was provided by the Arabidopsis Biological Resource Center (The Ohio State University, Columbus, OH, USA). This cDNA was used as a template to amplify the entire DNA-binding domain (DBD) of AtMYB30 by PCR using specific oligonucleotides. The forward primer contained a *Nde*I restriction site, AtMYB30 for (5'-GGA AAT CAT ATG GGA GTG AAG AAA GGG CC-3'), and the reverse primer contained the stop codon and a *Xho*I restriction site, AtMYB30 rev (5'-GTT AAC CTC GAG TTA GAG TTT CTT CTT CAA ATG AG-3'); the restriction sites are underlined. PCR amplification using Taq DNA polymerase consisted of an initial denaturation step at 95 °C for 5 min, followed by 30 cycles of denaturation at 95 °C for 45 s, annealing at 60 °C for 30 s, and extension at 72 °C for 1 min, with a final extension step at 72 °C for 10 min in the presence of 1.5 mM MgCl₂. The DNA fragment obtained (345 bp) was digested with *Nde*I and *Xho*I restriction enzymes and ligated into the pET-14b vector (Novagene) previously digested with the same enzymes. The fragment was inserted downstream and in-frame with a coding sequence corresponding to the following amino acid residues carrying a hexahistidine tag: MGSSHHHHHHSSGLVPRGSHM. The recombinant plasmid was used to transform *Escherichia coli* DH5 α competent cells. Clones carrying the pET14b-AtMYB30 recombinant plasmid were identified by colony PCR and checked by DNA sequencing. In order to express the recombinant AtMYB30 DBD, plasmid pET14b-AtMYB30 was used to transform *E. coli* BL21(DE3) pLysS. *E. coli* cells containing the pET14b-AtMYB30 recombinant plasmid were inoculated in 10 ml of LB containing ampicillin (100 μ g/ml) and chloramphenicol (50 μ g/ml). Overnight cultures were transferred to 250 ml of the same medium and were incubated at 37 °C under agitation until an OD value of 0.6 at 600 nm was reached.

Isopropyl- β -D-thiogalactopyranoside (IPTG) was added to a final concentration of 1 mM and cultures were further incubated at 15 °C for 15 h under agitation. Cells were harvested by centrifugation (5000 \times g for 30 min at 4 °C) and were resuspended in 3 ml of lysis buffer (50 mM sodium phosphate, pH 8.0) containing 300 mM NaCl, 10 mM imidazole and a protease inhibitor cocktail (Complete, Mini, Boehringer-Mannheim). The cells were disrupted by gentle sonication (6 cycles, 30 s) on ice and centrifuged (10,000 \times g for 30 min at 4 °C). AtMYB30 DBD was purified from the supernatant under native conditions by immobilized metal affinity chromatography (IMAC) in a HisTrap column (GE Healthcare Life Sciences) connected to an ÄKTA Purifier 900 system using a linear gradient of imidazole (0–500 mM). The purity of the protein preparation was assessed by SDS-PAGE in 16% acrylamide slab gels, under reducing conditions (Schägger and Von Jagow, 1987). The gels were stained with Coomassie brilliant blue R-250. The protein content was determined by the method of Bradford, with bovine serum albumin as standard [24].

2.2. Site-directed mutagenesis

Selected codons in the pET-14bAtMYB30 recombinant plasmid were mutated by PCR in order to obtain the following amino acid substitutions in AtMYB30 DBD: C49A, C53A and C49A/C53A. To substitute Cys 49 or Cys 53 to Ala, two rounds of PCRs were performed. In the first round, two halves of the AtMYB30 gene that carried overlapping sequences with the intended mutation introduced by each mutagenic primer were amplified (**AtMYB30 C49A DBD**: MUT49for 5'-GGG CTG CTT AGA GCT AGT AAG AGT-3' and MUT49rev 5'-ACT CTT ACT AGC TCT AAG CAG CCC-3'/**AtMYB30 C53A DBD**: MUT53for 5'-AGT AAG AGT GCT AGA CTT AGA TGG-3' and MUT53rev 5'-CCA TCT AAG TCT AGC ACT CTT ACT-3'/mutations introduced are underlined) [25]. MUT49for or MUT53for were used in association with AtMYB30Rev and MUT49rev or MUT53rev were used in association with AtMYB30For. The two mutated fragments obtained were then mixed and used as template in the second round of PCR in conjunction with primers AtMYB30For and AtMYB30Rev, under the conditions described before. The double mutant AtMYB30 C49A/C53A DBD was obtained in the same way, using AtMYB30 C53A DNA sequence as template. The DNA fragments obtained were digested with *Nde*I and *Xho*I restriction enzymes and ligated into the pET-14b vector previously digested with the same enzymes. The recombinant plasmids were used to transform *E. coli* DH5a competent cells. The mutations were verified by DNA sequencing. AtMYB30 mutant proteins were expressed and purified as described for wild type AtMYB30 DBD.

2.3. Electrophoretic mobility shift assay AACAAAC

DNA binding was monitored by electrophoretic mobility shift assay (EMSA) using the double-stranded oligonucleotide labeled probe (5'-/Alexa647N/CTTCTTTACTACCAACCTAACGGTCAACCAACCAACCTCTC-3') (MYB binding site with AC typical element is underlined) [5,15]. All binding reactions were performed in a total volume of 40 μ l. The reaction buffer contained 10 mM Tris-HCl (pH 7.5), 50 mM NaCl, 1 mM DTT, 1 mM EDTA, 5% glycerol and 0.4 μ M of the indicated proteins (wild type or mutants). Samples treated with the NO donor sodium nitroprusside (SNP, 1 mM) were incubated at 4 °C for 15 min. After treatment, the oligonucleotide probe (250 nM) was added and the binding mixture incubated for additional 15 min at 4 °C. The samples were analyzed by electrophoresis on a 10% native polyacrylamide gel, using a Tris-borate-EDTA (TBE) buffer system and visualized by fluorescence in a laser scanner Typhoon FLA9000 (GE Healthcare Life Sciences).

2.4. Biotin switch assay for detection of S-nitrosylated proteins

The protein concentration of the purified proteins in HEN buffer (Hepes 25 mM, pH 7.7; EDTA 1 mM) was adjusted to 0.5 mg/ml.

Samples (100 µl of each protein) were treated with 1 mM S-nitroso-N-acetylpenicillamine (SNAP) for 30 min at room temperature (RT) in the dark. After that, proteins were incubated for 30 min (RT) in 300 µl, 25 mM Hepes, pH 7.7 containing 1 mM EDTA; 3.3% (w/v) SDS, 27 mM MMTS (S-methyl methanethiosulfonate, alkylating reagent for Cys-SH). Samples were frequently vortexed to facilitate alkylation of non-nitrosylated, and reduced cysteine residues. A set of samples (control) was treated with the same volume of DMSO, instead of SNAP. Residual MMTS was removed by precipitation with 5 vol of chilled (−20 °C) acetone and the proteins were resuspended in 60 µl HEN buffer supplemented with 1% SDS. Biotinylation was achieved by adding 1 mM ascorbate and 2 mM biotin-HPDP, and incubating at room temperature for 1 h. To detect biotinylated proteins by western blot, samples from the biotin switch assay were separated on 10% SDS-PAGE gels, transferred to PVDF membranes, blocked with non-fat dried milk, and incubated with 1/10,000 mouse anti-biotin antibody (Sigma) for 1 h at 4 °C. Membranes were then washed and incubated for 1 h with anti-mouse IgG-peroxidase conjugate. Amersham ECL chemiluminescent kit was used to detect the signals and Typhoon FLA9000 (GE Healthcare Life Sciences) to visualize the results.

2.5. Mass spectrometry

Gel spots of purified proteins were repeatedly destained in 25 mM ammonium bicarbonate in 50% acetonitrile. The gel pieces were dehydrated with 100 µl of acetonitrile and then dried under vacuum (Concentrator Eppendorf, Hamburg, Germany). After drying, gel fragments were rehydrated on ice in 10 µl of sequencing grade modified trypsin (10 µg/ml in 25 mM ammonium bicarbonate (pH 8.0)) or LyS-C (5 µg/ml in 50 mM HEPES), 10 mM EDTA (pH 8.0) (Promega, Madison, WI) and incubated for 16 h at 37 °C. The resulting peptides were extracted with two washing steps (45 µl of 50% acetonitrile in 5% trifluoroacetic acid (TFA) for 30 min). Then, the concentrated peptide extracts were dried in a vacuum system. Extracted peptides were resuspended in 10 µl 0.1% TFA and a sample of 1 µl of the concentrated digest was mixed with 1 µl of a saturated matrix solution of α-cyano 4-hydroxycinnamic acid (5 mg/ml in 0.1% TFA and 50% acetonitrile). This mixture was spotted on the MALDI target plate (Bruker Daltonics, Bremen, Germany) and allowed to crystallize at RT. MS and MS/MS analysis were performed on a MALDI-TOF/TOF Autoflex III Smartbeam mass spectrometer (Bruker Daltonics, Bremen, Germany). The MS spectra were acquired in positive ion mode, using an accelerating voltage of 20 kV and laser frequency of 200 Hz. LIFT mass spectra were acquired in the positive ion mode. Metastable fragmentation was induced by a nitrogen laser

(337 nm) without acceleration to 6 kV and selected in a timed ion gate. In the LIFT-cell the fragments were further accelerated to 19 kV. External calibration was performed using peptide standards. The spectra generated were analyzed with FlexAnalysis 3.3 software (Bruker Daltonics, Bremen, Germany).

2.6. Purification of S-nitrosylated peptides and mass spectrometry

In vitro S-nitrosylation, and subsequent biotinylation of S-nitrosylated peptides was performed as described above. A neutravidin pull-down assay was used to purify biotinylated peptides. Briefly, after biotinylation, biotin-HPDP was removed by acetone precipitation, and the protein pellet was resuspended in 25 mM Tris HCl buffer and 1 mM EDTA, pH 7.7. Biotin switch-treated samples were digested using LyS-C endoprotease (Promega, Madison, WI), and incubated for 16 h at 37 °C. After cleavage, a total of 40 µl of neutravidin-agarose (Thermo Fisher Scientific) were added and incubated for 1 h at RT. The matrix was washed five times with 2 volumes of neutralization buffer (20 mM HEPES, pH 7.7, 100 mM NaCl, 1 mM EDTA, 600 mM NaCl and 0.5% Triton X-100) and bound peptides were eluted with neutralization buffer containing 100 mM β-mercaptoethanol. Then, the eluted peptides were concentrated under vacuum. A sample of 1 µl of the concentrated and purified peptides was mixed with 1 µl of a saturated matrix solution of α-cyano 4-hydroxycinnamic acid, and analyzed by mass spectrometry as described above.

2.7. Circular dichroism spectroscopy

Wild type AtMYB30 DBD and its mutants (10 µM) were dialyzed against buffer (10 mM Hepes, pH 7.4). Spectroscopic analyses were carried out in a JASCO J-815 spectropolarimeter equipped with a peltier temperature control unit. Circular dichroism was measured in a 0.2 cm pathlength cuvette (50 nm/min scan speed, response time 8 s, bandwidth 2 nm, data pitch 0.1 nm/s) with an average of 3 scans for each spectrum at a wavelength range from 190 nm to 260 nm. Thermal unfolding was carried out by increasing the temperature of the cuvette from 4 °C to 70 °C, and monitoring the 222 nm minimum peak. The effect of S-nitrosylation on protein thermal stability was assayed using GSNO as a NO donor, and glutathione as a negative control. The enzymes were pre-incubated with 1 mM GSNO or GSH for 30 min at 25 °C in the dark. In order to verify the reversibility of AtMYB30 DBD S-nitrosylation, the samples were incubated with 1 mM DTT after GSNO treatment. For all the scans recorded, the baseline spectrum containing only the buffer or buffer plus nitrosylating agents, and DTT were subtracted.

<i>M. musculus</i>	QNGTDDWKVIANYLPNRTDVQCQHRWQKVLNPELIKGPWTKCEDQRIELVQKYGPKRWS	116
<i>AtMYB30</i>	-----GVKKGPWTPPEEDIILVTYIQEHGPGNWR	38
<i>AtMYB2</i>	-----DVRKGPWTEEDAILVNFVSIHGDAWN	46
<i>O. sativa</i>	PQGEDPLIG-----IKAAAAGGGIMRKGPWTEQEDVQLVWFVRLGERRWD	82
	***** ** *	
<i>M. musculus</i>	VIAKHL-KGRIGKQCRERWHNHLNPEVKKTS-----TEEDRIIYQAHKRLGN	163
<i>AtMYB30</i>	AVPTNTGLLRCSKSCRLRWNTYLRPGIKRGN-----FTEHEEKMIHVHLQALLGN	87
<i>AtMYB2</i>	HIARSSGLKRTGKSCRLRWNTYLRPDVRRGN-----ITLLEQFMILKLHSLWGN	95
<i>O. sativa</i>	FLAKVSGLQRSKSCRLRWNTYLRHPLKRG-----MSPEEERMVVLHAKLGN	131
	* * * * *	
<i>M. musculus</i>	RWAEIAKLLPGRTDNAIKHNWNTMRRKVEQEGYLQEPKASQTPV-----A-----	210
<i>AtMYB30</i>	RWAAIASYLPQRTDNDIKNYWNTHLKKKL-----	116
<i>AtMYB2</i>	RWSKIAQYLPGRTDNEIKNYWRTRVQKQAK-----	125
<i>O. sativa</i>	RWSRIAKSIPGRTDNEIKNYWTRHLRKLKLKQKQKQSDHNDND-----DDDDRNSS	185
	** ** * * * *	

Fig. 1. DNA binding domain sequence alignment of *Arabidopsis thaliana* AtMYB30 (AF250339.1) with MYB factors from a typical plant model (AAU84433.1), AtMYB2 (NP_182241.1), and mammal (NP_034978.3). Asterisks indicate conserved amino acid residues, and the peptides identified in wild type AtMYB30 by mass spectrometry are underlined. Numbers at the right are indicative of the position of the amino acid residue in the complete protein sequence.

3. Results and discussion

In Fig. 1, a primary sequence comparison between DNA binding domains of AtMYB30, AtMYB2, and MYB transcription factors from *Oryza sativa*, and *Mus musculus* is depicted, to confirm the similarity observed in the DNA binding domain of these transcription factors from divergent species. We also stress the fact that the C49 residue is present only in AtMYB30, although the C53 is clearly conserved among MYB factors. Wild type AtMYB30 DBD and cysteine single and double mutants were expressed in *E. coli* strain BL21(DE3) pLysS after 15 h induction with 1 mM IPTG at 15 °C. The bacterial lysate was incubated and treated as described in Materials and methods. The protein yield was approximately 4 mg/l of cell culture for wild type and single mutants and 2 mg/l for the double mutant. The protein preparations obtained were homogeneous as judged by SDS-PAGE, producing a single band with an apparent molecular mass of 15 kDa (Fig. 2), consistent with the theoretical molecular mass (~14,600 Da) predicted for the full-length recombinant proteins.

The identity of the purified wild type AtMYB30 DBD and mutants was ascertained by MALDI mass spectrometry. The tryptic digest was consistent with the expected molecular masses of theoretical peptides and covered 75%, 74%, 53% and 50% of the DBD complete amino acid sequence, for wild type, C49A, C53A and C49A/C53A, respectively (data not shown).

We also checked the intact mass of the proteins to verify the integrity of the recombinant constructs. MALDI mass spectrometry of all recombinant proteins was consistent with the theoretical molecular mass (wild type, 14,647.7 Da; C49A and C53, 14,615.6 Da; and C49/53A, 14,583.6 Da) predicted for the full-length proteins (Fig. S1). It is

important to note that we detected the loss of the first methionine residue in each full-length protein due to the amino terminal peptidase activity, as described [26].

3.1. DNA binding activity of wild type AtMYB30, C49A, C53A, and C49A/C53A DNA binding domains

In order to analyze the DNA binding activity of AtMYB30 DBD and the potential effect of nitrosylation on cysteine residues we used the electrophoresis mobility shift assay (EMSA) technique. The AtMYB30 DBD and mutants C49A and C53A retarded the migration of a double-stranded oligonucleotide containing the binding sequence 5'-ACAA AAC-3' (Fig. 3), confirming that the DNA binding module of AtMYB30 (residues 11–116) is sufficient to target and bind DNA. The single site mutations (C49A or C53A) did not alter the binding activity of AtMYB30, but the double mutant (C49/53A) was clearly affected in its function, being unable to interact with DNA. Interestingly, treatment of wild type AtMYB30 DBD or any of the two single cysteine mutants with the NO donor sodium nitroprusside (SNP, 1 mM) before the addition of the specific DNA probe, completely abolished the formation of a protein–DNA complex (Fig. 3), other NO donors promote similar effects (Fig. S4). This effect was reversed by the addition of 50 mM DTT after the initial NO exposure. These results indicate the reversibility of the NO modification, in accordance with previous reports with similar transcription factors [1,8,9]. In addition, the double mutant C49A/C53A was unable to interact with the specific double-stranded oligonucleotide probe indicating that the absence of both cysteine residues abolishes complex formation (Fig. 3).

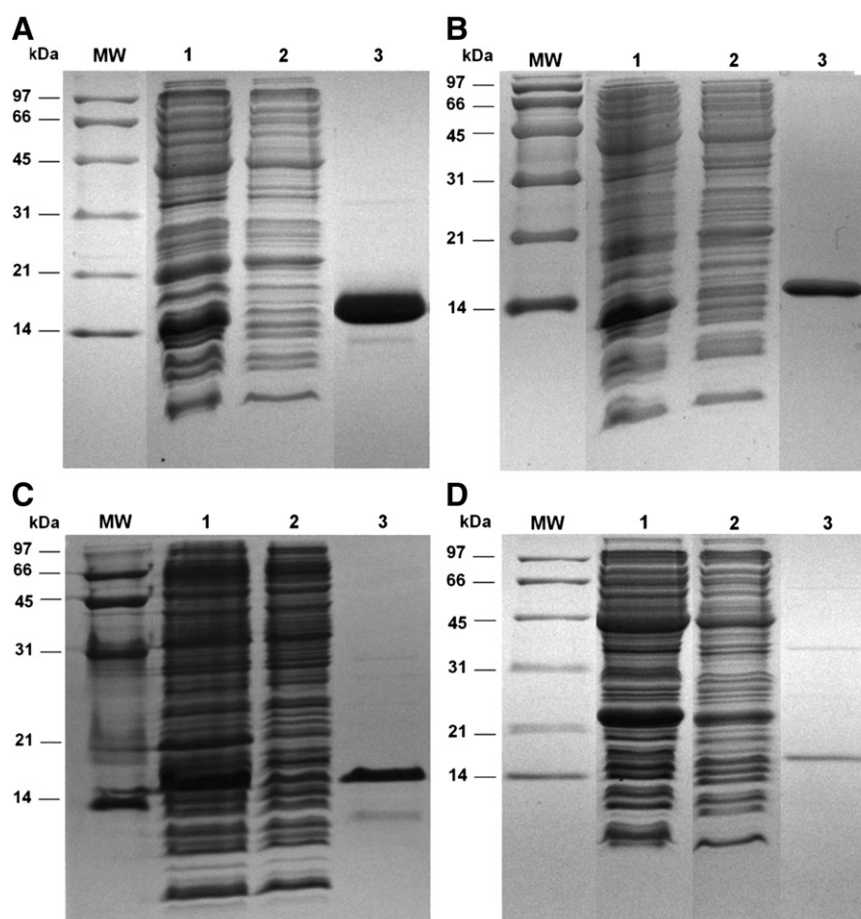


Fig. 2. Purification of recombinant wild type AtMYB30 (DBD) (20 µg) (A), mutant C49A (10 µg) (B), mutant C53A (10 µg) (C) and mutant C49A/C53A (3 µg) (D). SDS-PAGE following purification by affinity chromatography. 1 – Supernatant after sonication; 2 – Flow-through; and 3 – Proteins eluted with imidazole.

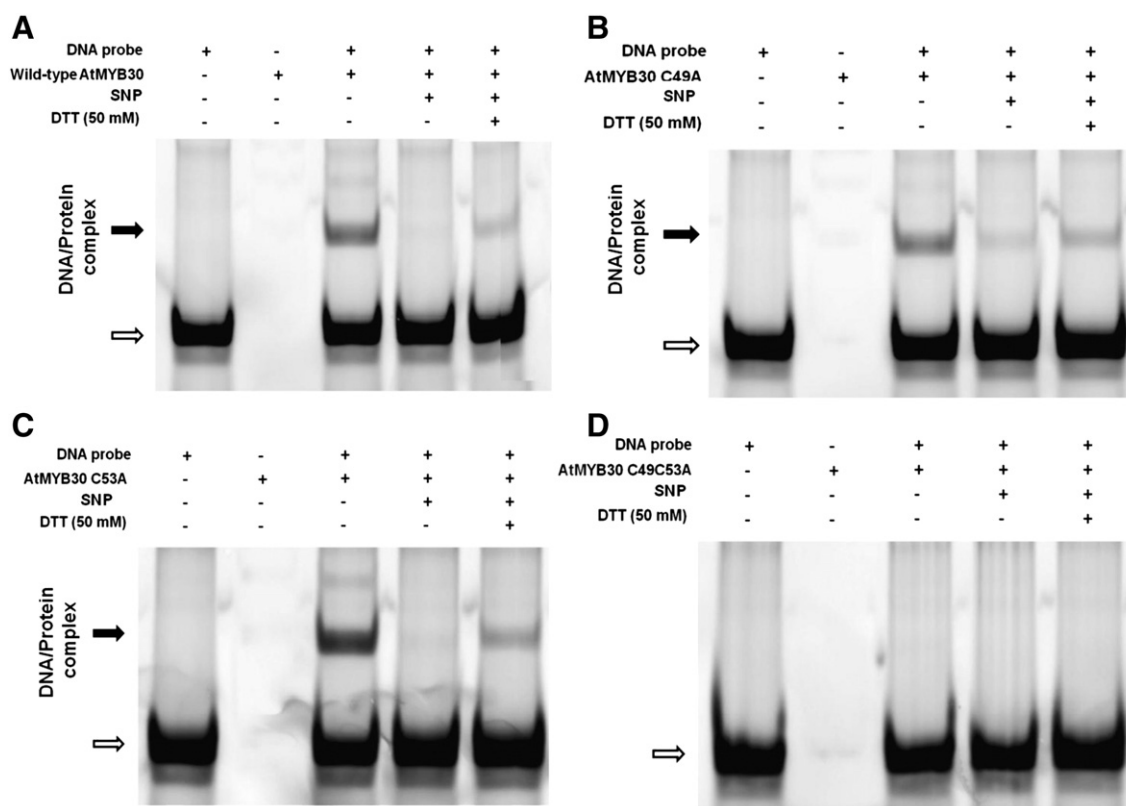


Fig. 3. Gel mobility shift assay of wild type AtMYB30 DBD (A), C49A (B), C53A (C) and C49A/C53A (D) using specific DNA probe. Filled and open arrows indicate protein–DNA complex and free DNA probe, respectively.

All these results indicate that a minimal AtMYB30 DNA-binding domain, spanning residues 11–116 is functionally active, as well as the single mutant proteins. The binding to DNA is strongly inhibited by nitrosylating agents, such as SNP, and the inhibition of the DNA-binding activity for wild type AtMYB30, C49A and C53A mutants was reversed by DTT, indicating that C49 and C53 reduced state is necessary for DNA-binding activity. These results suggest that DNA-binding activity of wild type AtMYB30, and its single mutants is probably regulated by S-nitrosylation, as our group observed for AtMYB2 DBD [9]. These findings are also in agreement with the fact that S-nitrosylation is emerging as a prototypic redox-based post-translational modification regulated by S-nitrosoglutathione (GSNO) reductase, the major

regulator of total cellular SNO levels in plants [27]. Besides, Yun and co-workers obtained genetic evidences supporting that the increment in cysteine thiols modified by NO facilitates the HR in the absence of the cell death agonist salicylic acid, a signaling molecule that is produced in the initial steps after plant–pathogen interaction [12]. Due to the close proximity of the two cysteines residues in wild type AtMYB30 DBD (C49 and C53) we investigated the existence of a possible disulfide bond between these residues, and whether this bond could affect the formation of DNA–protein complex. Thus the proteins were incubated with 5 mM of either reducing agent DTT or GSH before the addition of DNA probe (Fig. 4). We observed that the DNA–protein complex is formed even after the treatment of AtMYB30 DBD with reducing agents,

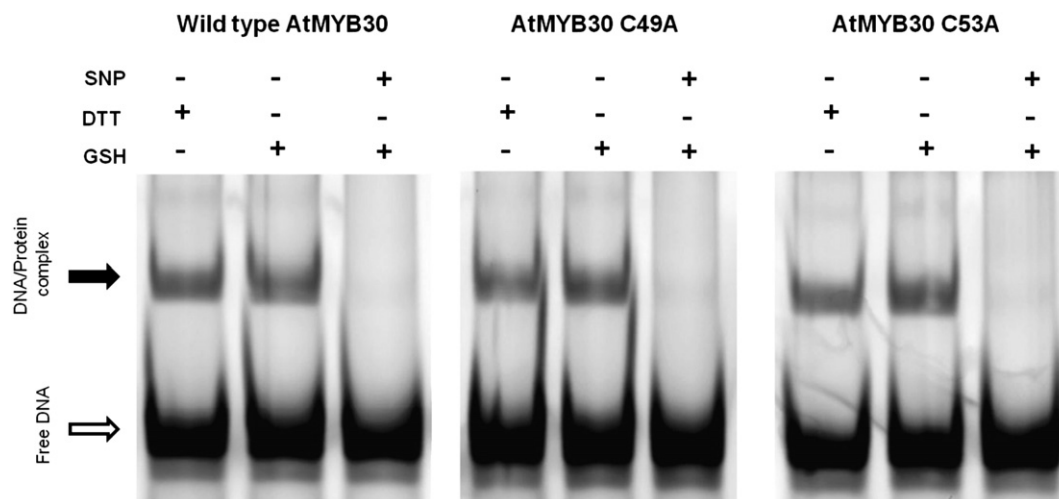


Fig. 4. Gel mobility shift assay of wild type AtMYB30 DBD, AtMYB30 C49A, and AtMYB30 C53A using specific DNA probe. All proteins were previously incubated with DTT or GSH 5 mM before addition of the DNA probe. Filled and open arrows indicate protein–DNA complex and free DNA probe, respectively. SNP, sodium nitroprusside NO donor.

suggesting that a putative disulfide bond between cysteines C49 and C53 is not required for DNA binding.

3.2. S-Nitrosylation of AtMYB30 as a consequence of NO treatment

Based on the results discussed above we investigated the S-nitrosylation of wild type AtMYB30 DBD and mutants C49A, C53A, and C49A/C53A using the biotin switch technique (BST) [28], to fully understand the role of each residue in the NO modification.

We observed that wild type AtMYB30 DBD and mutants C49A and C53A were S-nitrosylated by the NO donor SNAP, when compared with the negative control (DMSO) (Fig. 5). Similar results were obtained using GSNO and SNP as NO donors (data not shown). This suggests that both cysteine residues present in the DNA binding domain of AtMYB30 (C49 and C53) are targets for NO mediated S-nitrosylation.

We also detected the nitrosylation of AtMYB30 DBD by mass spectrometry (Figs. S2 and S3), the peptide containing C53 residue (1920 m/z; modified by iodoacetamide) was sequenced and its identity confirmed. We thus treated AtMYB30 DBD with a NO donor, and submitted the sample to the biotin-switch assay. Subsequently the samples were digested with LysC protease, in order to obtain the C53 containing peptide, and finally, the biotinylated peptides were isolated by neutravidin-agarose chromatography. As shown in Fig. S3, the C53 containing peptide was enriched after NO donor treatment, thus confirming its NO modification.

3.3. Effect of S-nitrosylation in the secondary structure of wild type AtMYB30 DBD and mutants C49A and C53A

We used circular dichroism (CD) spectroscopy to analyze the possible structural modification caused by site-directed mutagenesis in the Cys-mutants (Fig. 6). The CD data obtained for wild type AtMYB30 DBD and single mutants exhibit a typical α -helical secondary structure profile with minimal peaks at 208 nm and 222 nm. It is possible to observe that the substitution of Cys49 or Cys53 by alanine did not change the spectral profile (Fig. 6). Thus, the single mutations do not interfere directly in the secondary structure of the recombinant proteins.

Besides, in order to evaluate the structural stability of AtMYB30 DBD upon S-nitrosylation, CD spectra were obtained with wild type AtMYB30 DBD and Cys-mutants. When the NO donor (GSNO) was added to wild type AtMYB30 DBD or single mutants, the overall far-UV spectrum changed (Fig. 7), indicating that S-nitrosylation of each protein interferes with their secondary structure profile. It is important

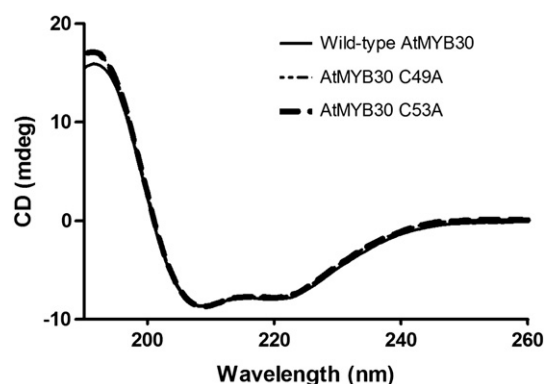


Fig. 6. Circular dichroism spectroscopy in the far-UV spectral region of wild type AtMYB30 DBD and single Cys mutants. The measurements were done with 10 mM protein in 10 mM Hepes, pH 7.4. The spectra represent the average of three scans and data represent a mean of three independent experiments.

to note that after DTT treatment, the original profile of the proteins treated with GSNO is partially restored, suggesting the reversibility of C49 and C53 S-nitrosylation (Fig. 7). It is also possible to assume that the effect of NO in the CD spectra is more pronounced in the C53A mutant, possibly indicating that modification of C49 causes a mild structural effect in AtMYB30 DBD. From this data we suggest that, although both C49 and C53 are potentially S-nitrosylated, C49 seems to be more important to the structural modification of the C53A mutant.

The thermal denaturation of proteins can be monitored by circular dichroism and it is normally used to determine the stability of a protein. In this case the thermal denaturation profile of AtMYB30 DBD indicated a melting temperature (T_M) of 38.26 °C while C49A and C53A mutants were less stable, and a lower melting temperature was observed for them (32.43 °C and 31.25 °C, respectively) (Fig. 8).

On the other hand, when wild type AtMYB30 DBD was S-nitrosylated, the thermal denaturation profile indicated a slight increase of 3.69 ± 1.01 °C in the melting temperature when compared to the non-nitrosylated enzyme (Fig. 9) and the melting temperature of C49A also increased in the presence of GSNO (from 33.08 to 39.82; ~ 6 °C). It is important to note that only for C53A mutant the T_M decreased in the presence of GSNO (from 29.49 to 23.15), refer to Fig. 9 and Table 1. Once more, as indicated above for the effect of nitrosylation on the overall CD spectra, the S-nitrosylation of the C49 residue (present in the C53A mutant) promoted the most pronounced effect — thermal

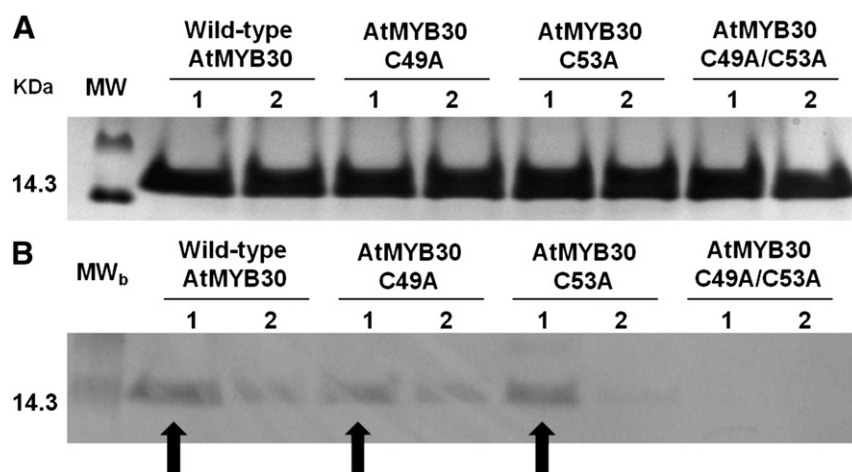


Fig. 5. S-nitrosylation of AtMYB30 DBD detected by the biotin switch technique. (A) Fifty micrograms of the indicated purified recombinant proteins were treated separately with 1 mM SNAP (1) or 1 mM DMSO (2) as negative control, separated by SDS-PAGE and stained with Coomassie blue. (B) Detection of S-nitrosylated proteins wild type AtMYB30 DBD, C49A, C53A and C49A/C53A. The relative molecular mass of the protein standard is shown on the left.

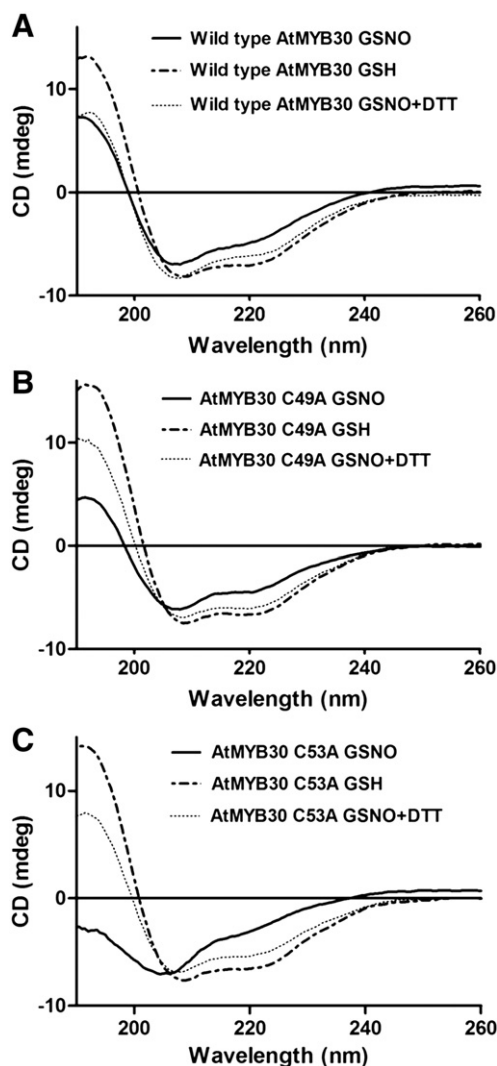


Fig. 7. Circular dichroism spectroscopy in the far-UV spectral region of wild type AtMYB30 DBD (A), C49A (B) and C53A (C) after GSH, GSNO or GSNO and DTT treatment. The spectra represent the average of three scans and data represent a mean of three independent experiments.

sensitivity. The opposing result (higher thermal stability upon nitrosylation) was detected in wild type and C49A mutant. We then suggest that residue C49 may be responsible for the NO structural modifications. These results support the evidence that the surrounding environment of cysteine residues in proteins affects the reactivity to NO [29,30].

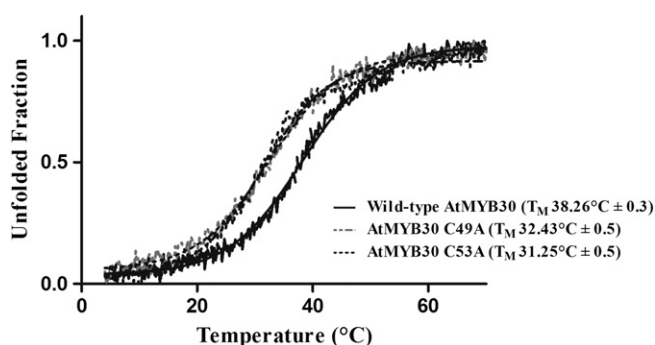


Fig. 8. Boltzmann sigmoidal curve showing unfolding (%) of wild type AtMYB30 DBD, C49A and C53A. Data represent a mean of three independent experiments.

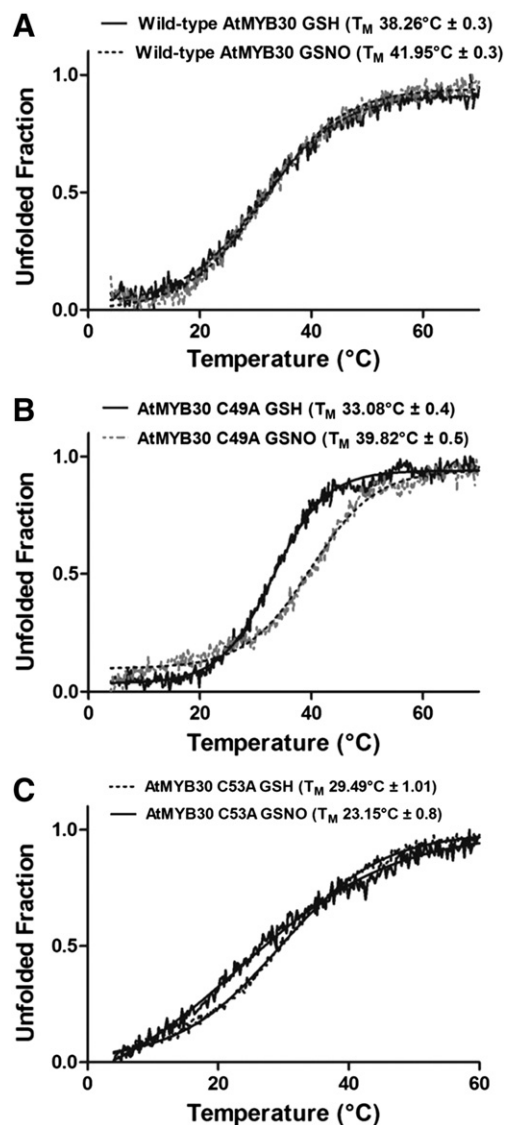


Fig. 9. Boltzmann sigmoidal curve showing unfolding (%) of wild type AtMYB30 DBD (A), C49A (B) and C53A (C) after GSH or GSNO treatment. Data represent a mean of three independent experiments.

4. Conclusions

Using techniques such as biotin switch, CD, and EMSA we observed that AtMYB30 Cys49 and Cys53 were nitrosylated by 1 mM SNAP, inhibiting DNA binding. By site-directed mutagenesis of cysteine residues it was possible to confirm that the nitrosylation occurs in these specific amino acid residues. The DNA–protein interaction was also strongly inhibited by another nitrosylating agent, such as SNP, and the inhibition of the DNA-binding activity for wild type and mutants was

Table 1

Average values of T_M (°C) of WT AtMYB30 and mutants after treatment with GSH (1 mM) or GSNO (1 mM).

Proteins		Melting temperature (T_M)
Wild-type AtMYB30	Non-nitrosylated	38.26 °C ± 0.3
	Nitrosylated	41.95 °C ± 0.3
AtMYB30 C49A	Non-nitrosylated	33.08 °C ± 0.4
	Nitrosylated	39.82 °C ± 0.5
AtMYB30 C53A	Non-nitrosylated	29.49 °C ± 1.01
	Nitrosylated	23.15 °C ± 0.8

reversed by DTT, suggesting that Cys49 and Cys53 are S-nitrosylated and the reduced state is necessary for DNA-binding activity. Besides, using circular dichroism we observed that S-nitrosylation affects the secondary structure of AtMYB30 DBD and mutants C49A and C53A. All these results suggest that nitrosylation is one of the mechanisms driving the NO-mediated inhibition of AtMYB30 DBD binding to DNA. Our findings underline the importance of this modification for AtMYB30 and support other evidences that S-nitrosylation is an important and widespread regulator of protein function in plant biology. It has been demonstrated that AtMYB30 is a positive regulator of the hypersensitive response (HR) which is accompanied by a burst of reactive oxygen and nitrogen species leading to cell death in plants [16], and that in non-infected plants, AtMYB30 is ubiquitinated by the E3 ligase MIEL1 triggering its proteasomal degradation and thus, attenuating the HR. We may speculate that the S-nitrosylation of AtMYB30 and the subsequent inhibition of its binding to DNA may be operating during the HR to limit the damage of an extensive and uncontrolled cell death triggered by a hyperactive AtMYB30. This is the second observation of a MYB transcription factor in *A. thaliana* to be inhibited by NO action. Indeed, it was recently reviewed [31] that growing evidence indicates AtMYB30 as a multi-regulated protein linked to diverse environmental stimuli response, acting as a major regulator of plant responses and subjected to many different post-translational modifications (phosphorylation, sumoylation, ubiquitination). This work brings evidence of a fourth covalent modification in AtMYB30, at least 'in vitro'.

Appendix A. Supplementary data

Supplementary data to this article can be found online at <http://dx.doi.org/10.1016/j.bbapap.2014.02.015>.

References

- [1] L. Zhang, G. Zhao, J. Jia, X. Liu, X. Kong, Molecular characterization of 60 isolated wheat MYB genes and analysis of their expression during abiotic stress, *J. Exp. Bot.* 63 (2012) 203–214.
- [2] A. Feller, K. Machemer, E.L. Braun, E. Grotewold, Evolutionary and comparative analysis of MYB and bHLH plant transcription factors, *Plant J.* 66 (2011) 94–116.
- [3] T. Mengiste, X. Chen, J. Salmeron, R. Dietrich, The botrytis susceptible 1 gene encodes an R2R3MYB transcription factor protein that is required for biotic and abiotic stress responses in *Arabidopsis*, *Plant Cell* 15 (2003) 2551–2565.
- [4] C. Dubos, R. Stracke, E. Grotewold, B. Weisshaar, C. Martin, L. Lepiniec, MYB transcription factors in *Arabidopsis*, *Trends Plant Sci.* 15 (2010) 573–581.
- [5] M.B. Prouse, M.M. Campbell, The interaction between MYB proteins and their target DNA binding sites, *Biochim. Biophys. Acta* 1819 (2012) 67–77.
- [6] J.L. Riechmann, J. Heard, G. Martin, L. Reuber, C. Jiang, J. Keddie, L. Adam, O. Pineda, O.J. Ratcliffe, R.R. Samaha, R. Creelman, M. Pilgrim, P. Broun, J.Z. Zhang, D. Ghandehari, B.K. Sherman, G. Yu, *Arabidopsis* transcription factors: genome-wide comparative analysis among eukaryotes, *Science* 290 (2000) 2105–2110.
- [7] C. Lindermayr, J. Durner, S-Nitrosylation in plants: pattern and function, *J. Proteomics* 73 (2009) 1–9.
- [8] E.M. Brendeford, K.B. Andersson, O.S. Gabrielsen, Nitric oxide (NO) disrupts specific DNA binding of the transcription factor c-Myb *in vitro*, *FEBS Lett.* 425 (1998) 52–56.
- [9] V. Serpa, J. Vernal, L. Lamattina, E. Grotewold, R. Cassia, H. Terenzi, Inhibition of AtMYB2 DNA-binding by nitric oxide involves cysteine S-nitrosylation, *Biochem. Biophys. Res. Commun.* 361 (2007) 1048–1053.
- [10] S. Grun, C. Lindermayr, S. Sell, J. Durner, Nitric oxide and gene regulation in plants, *J. Exp. Bot.* 57 (2006) 507–516.
- [11] J. Astier, S. Rasul, E. Koen, H. Manzoor, A. Besson-Bard, O. Lamotte, S. Jeandroz, J. Durner, C. Lindermayr, D. Wendehenne, S-nitrosylation: an emerging post-translational modification in plants, *Plant Sci.* 181 (2011) 527–539.
- [12] B.-W. Yun, A. Feechan, M. Yin, N.B.B. Saidi, T.L. Bihan, M. Yu, J.W. Moore, J.-G. Kang, E. Kwon, S.H. Spoel, J.A. Pallas, G.J. Loake, S-nitrosylation of NADPH oxidase regulates cell death in plant immunity, *Nature* 478 (2011) 264–268.
- [13] S. Guehmann, G. Vorbruggen, F. Kalkbrenner, K. Moelling, Reduction of a conserved Cys is essential for Myb DNA-binding, *Nucleic Acids Res.* 20 (1992) 2279–2286.
- [14] X. Daniel, C. Lacomme, J.-B. Morel, D. Roby, A novel myb oncogene homolog in *Arabidopsis thaliana* related to the hypersensitive cell death, *Plant J.* 20 (1999) 57–66.
- [15] L. Li, X. Yu, A. Thompson, M. Guo, S. Yoshida, T. Asami, J. Chory, Y. Yin, *Arabidopsis* MYB30 is direct target of BES1 and cooperates with BES1 to regulate brassinosteroid-induced gene expression, *Plant J.* 58 (2009) 275–286.
- [16] D. Marino, S. Froidure, J. Canonne, S. Ben Khaled, M. Khaffif, C. Pouzet, A. Jauneau, D. Roby, S. Rivas, *Arabidopsis* ubiquitin ligase MIEL1 mediates degradation of the transcription factor MYB30 weakening plant defense, *Nat. Commun.* 4 (2013) 1476.
- [17] S. Raffaele, S. Rivas, D. Roby, An essential role for salicylic acid in AtMYB30-mediated control of the hypersensitive cell death program in *Arabidopsis*, *FEBS Lett.* 580 (2006) 3498–3504.
- [18] S. Raffaele, F. Vaillau, A. Leger, J. Joubes, O. Miersch, C. Huard, E. Blee, S. Mongrand, F. Domergue, D. Roby, A MYB transcription factor regulates very-long-chain fatty acid biosynthesis for activation of the hypersensitive cell death response in *Arabidopsis*, *Plant Cell* 20 (2008) 752–767.
- [19] Y. Zheng, K.S. Schumaker, Y. Guo, Sumoylation of transcription factor MYB30 by the small ubiquitin-like modifier E3 ligase SIZ1 mediates abscisic acid response in *Arabidopsis thaliana*, *Proc. Natl. Acad. Sci. U. S. A.* 109 (2012) 12822–12827.
- [20] S. Froidure, J. Canonne, X. Daniel, A. Jauneau, C. Brière, D. Roby, S. Rivas, AtsPLA2- α nuclear relocalization by the *Arabidopsis* transcription factor AtMYB30 leads to repression of the plant defense response, *Proc. Natl. Acad. Sci. U. S. A.* 107 (2010) 15281–15286.
- [21] J. Canonne, D. Marino, A. Jauneau, C. Pouzet, C. Brière, D. Roby, S. Rivas, The Xanthomonas type III effector XopD targets the *Arabidopsis* transcription factor MYB30 to suppress plant defense, *Plant Cell* 23 (2011) 3498–3511.
- [22] J. Astier, C. Lindermayr, Nitric oxide dependent posttranslational modification in plants: an update, *Int. J. Mol. Sci.* 13 (2012) 15193–15208.
- [23] M. Yu, B.W. Yun, S.H. Spoel, G.J. Loake, A sleigh ride through the SNO: regulation of plant immune function by protein S-nitrosylation, *Curr. Opin. Plant Biol.* 15 (2012) 424–430.
- [24] M.M. Bradford, A rapid and sensitive method for the quantitation of microgram quantities of protein utilizing the principle of protein-dye binding, *Anal. Biochem.* 72 (1976) 248–254.
- [25] M.M. Ling, B.H. Robinson, Approaches to DNA mutagenesis: an overview, *Anal. Biochem.* 254 (1997) 157–178.
- [26] Q. Xiao, F. Zhang, B.A. Nacev, J.O. Liu, D. Pei, Protein N-terminal processing: substrate specificity of *Escherichia coli* and human methionine aminopeptidases, *Biochemistry* 49 (2010) 5588–5599.
- [27] E. Kwon, A. Feechan, B.W. Yun, B.H. Hwang, J.A. Pallas, J.G. Kang, G.J. Loake, AtGSNOR1 function is required for multiple developmental programs in *Arabidopsis*, *Planta* 236 (2012) 887–900.
- [28] S.R. Jaffrey, S.H. Snyder, The biotin switch method for the detection of S-nitrosylated proteins, *Sci. STKE* 86 (2001) p1.
- [29] D. Spadaro, B.W. Yun, S.H. Spoel, C. Chu, Y.Q. Wang, G.J. Loake, The redox switch: dynamic regulation of protein function by cysteine modifications, *Physiol. Plant.* 138 (2010) 360–371.
- [30] S.M. Marino, V.N. Gladyshev, Structural analysis of cysteine S-nitrosylation: a modified acid-based motif and the emerging role of trans-nitrosylation, *J. Mol. Biol.* 395 (2010) 844–859.
- [31] S. Raffaele, S. Rivas, Regulate and be regulated: integration of defense and other signals by the AtMYB30 transcription factor, *Front. Plant Sci.* 4 (2013) 1–7.